THE PENNSYLVANIA STATE UNIVERSITY

IONOSPHERIC RESEARCH

Scientific Report No. 230

THE REDUCTION OF IONOGRAMS FROM THE BOTTOMSIDE AND TOPSIDE

by

J. R. Doupnik

and

E. R. Schmerling

January 1, 1965

IONOSPHERE RESEARCH LABORATORY

University Park, Pennsylvania NASA Grant No. NsG-134-61

Ionospheric Research

NASA Grant No. NsG-134-61

Scientific Report

on

"The Reduction of Ionograms from the Bottomside and Topside"

by

J. R. Doupnik
and
E. R. Schmerling

January 1, 1965

Scientific Report No. 230

Ionosphere Research Laboratory

Submitted by: _____
J. S. Nisbet, Associate Professor of Electrical Engineering
Project Supervisor

Approved by: _____
A. H. Waynick, Director, Ionosphere Research Laboratory

The Pennsylvania State University
College of Engineering
Department of Electrical Engineering

Table of Contents

ABSTRACT

19688

A method is discussed for reducing ionograms to electron density height profiles on a modern digital computer by a representation in terms of parabolic laminations. This provides good accuracy without an excessive number of scaled points. Since no precomputed coefficients are used, ionograms may be scaled at any frequency and from any location. It is shown how a least squares joint ordinary and extraordinary analysis enable a correction to be made for underlying ionization, and reduces sensitivity to scaling errors.

Some special features of topside ionograms are discussed. Formulation in terms of segments parabolic in log (plasma frequency) is especially efficient in terms of matching layer shape without discontinuity of slope. Techniques for incorporating the variation of gyrofrequency with altitude are discussed. It is particularly emphasized that significant errors in the deduced electron scale height can be made if this is not done adequately.

Author

1. INTRODUCTION

The sweep frequency ionosonde provides a powerful tool for obtaining electron density profiles in the ionosphere, particularly in the F region. In recent years, not only have ground based ionosondes been used for profiles up to the F region electron peak, but topside sounders have also been used in an analogous manner to obtain profiles from satellite altitudes down to the peak of the F region. Unfortunately, the reduction of these ionograms to electron profiles is not always a straight forward matter, and a number of methods have been described in the literature for accomplishing this with varying degrees of ease and accuracy.

In this work, a versatile method is developed for use on a high speed digital computer. Full account is taken of the earth's magnetic field, and the ionograms may be scaled at any frequency and for any geographical location since no precomputed coefficients are used. The method is based on fitting the profile by a set of parabolic laminations, which provide more accuracy than linear laminations without the danger of oscillation inherent in higher order polynomials. Conversely, for a given accuracy, fewer points need to be scaled. Discussion is restricted to the case of monotonic profiles.

It is shown how the method may be extended to a joint reduction of ordinary and extraordinary traces, and how the use

of a least squares technique reduces sensitivity to scaling errors. With this approach, a correction for low frequency cut-off errors using average values of a low frequency virtual height is shown to be quite feasible for the F region.

The topside presents some special features. Advantage is taken of the approximately logarithmic shape expected from theory and found in practice. On the other hand, account must be taken of the variation of gyrofrequency with altitude. Several methods of doing this are discussed, and a model study illustrates the errors which can arise both in the profile and the deduced values of electron scale height. It is shown that significant errors in this scale height can result from an inadequate method for compensating for this variation.

2. SINGLE MODE ANALYSIS

The electron density profile is represented by a set of parabolic segments of the form

$$Z = Z_j + a_j (f_N - f_{N_j}) + b_j (f_N - f_{N_j})^2; \quad f_{N_j} \leq f_N \leq f_{N_{j+1}} \qquad (1)$$

as illustrated in Figure 1. Each parabola extends between two plasma frequencies, f_{N_j} and $f_{N_{j+1}}$. These are the reflection frequencies for which the ordinary or extraordinary rays are

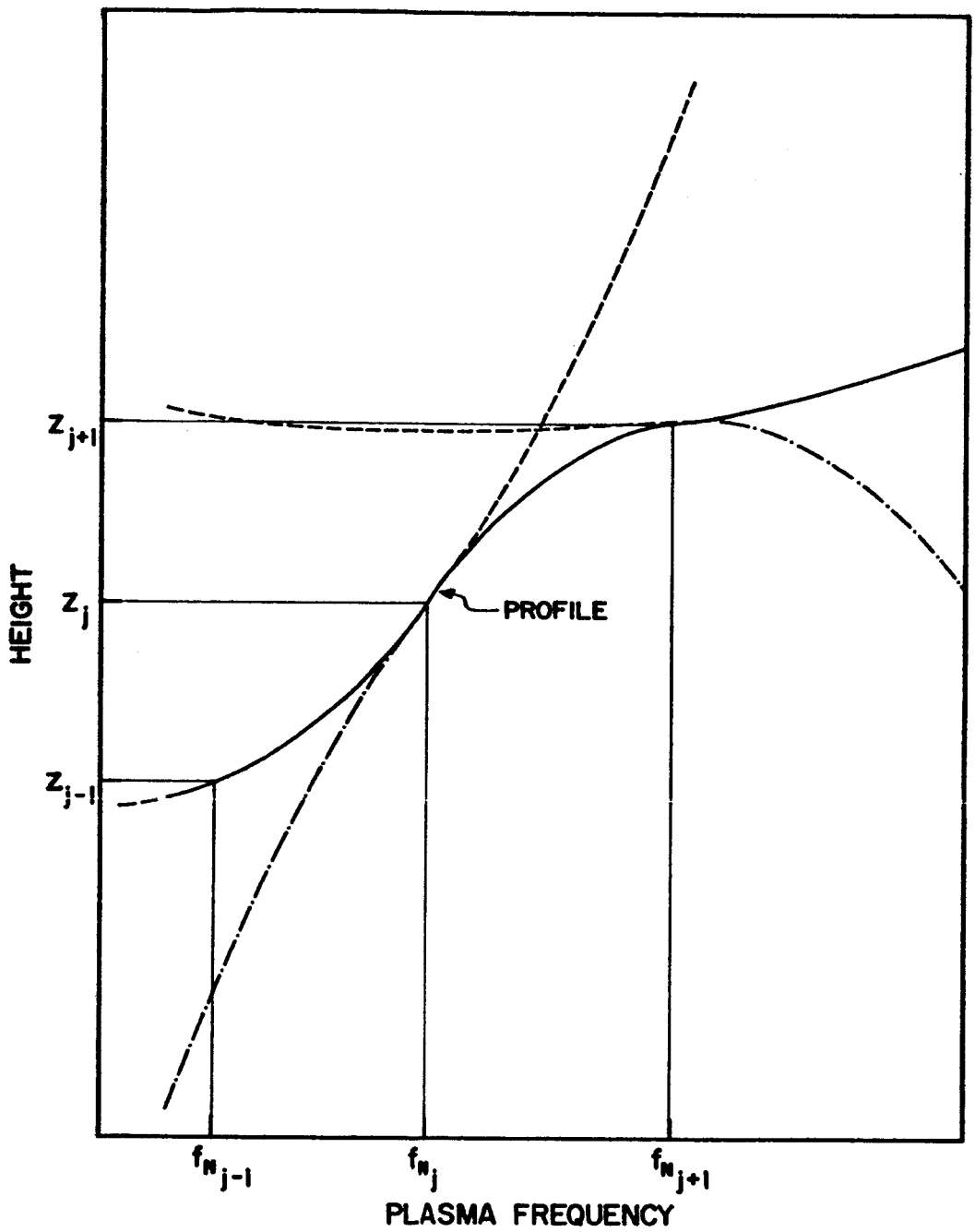

REPRESENTATION OF AN ELECTRON DENSITY PROFILE (CONTINUOUS LINE) BY PARABOLIC SEGMENTS (BROKEN LINES)

FIGURE 1

scaled and can be chosen at will. The parabolic segments are constrained to have continuity of height and slope at their junction. Therefore, Z_j is known from the previous segment and

$$a_j = a_{j-1} + 2b_{j-1}(f_{N_j} - f_{N_{j-1}}) . \tag{2}$$

Thus, there are three unknowns: Z_1, a_1, and b_1 for the first segment, but there is only one unknown, b_j, for each of the others.

Equation (1) can also be derived by expanding Z in a Taylor series about f_{N_j} up to the second derivative. In this form the present method is similar to that of Paul (1960 a,b) who used an expansion in f_N^2. In the well-known method of Budden (1954), linear segments are employed, and Titheridge (1961) has used polynomials of higher degree over much longer intervals. There is no "best" choice of functions below the F2 peak because of the complicated structure of the lower ionosphere.

The well known equation relating true height, Z, to virtual height, h', for a monotonic profile is

$$h'(f_k) = Z_1 + \int_o^{f_{N_k}} \mu' \frac{dZ}{df_N} \, df_N \tag{3}$$

where μ' is the group refractive index of either the ordinary or extraordinary mode, and Z_1 is the effective base of the ionosphere

where $f_N = 0$. The plasma frequencies of reflection, f_{N_k}, are given by

$$f_{N_k} = f_k \text{ for the ordinary mode,}$$

and $$f_{N_k} = \sqrt{f_k^2 - f_k f_N} \text{ for the extraordinary mode,}$$

where f_h is the electron gyrofrequency.

Combining equations (1) and (3) gives

$$h'(f_k) = Z_1 + \sum_{j=1}^{k-1} \left[a_j \int_{f_{N_j}}^{f_{N_{j+1}}} \mu' \, df_N + 2b_j \int_{f_{N_j}}^{f_{N_{j+1}}} (f_N - f_{N_j}) \, \mu' \, df_N \right]. \quad (4)$$

These integrals can be calculated immediately in a straight forward manner as described in Appendix 1. If the term in b_j is put equal to zero, this reduces to the linear segment method of Budden. It is interesting to note that the extra term needed here can be obtained with only a trivial increase in machine time, since most of this time is needed for computing μ' which is used in evaluating both integrals simultaneously.

To solve equation (4) for the first segment, the additional constants Z_1 and a_1 must be found by an alternative method since there is only one virtual height available here. This can be done in a variety of ways, one of which is to compute the first parabola from the first three virtual heights. Table 1 shows the results obtained from a model computation for the cosine layer defined by

Table 1

Constants for First Segment in Equation (4) for a Given Model

Cosine model		Parabolic method				Budden method			
		10 pts		5 pts		10 pts		5 pts	
f_N (mc)	height (km)	O	X	O	X	O	X	O	X
0.0	0.0	0.0	0.0	0.0	0.0	0.0	0.0	0.0	0.0
0.5	8.49	8.49	8.48			8.56	8.56		
1.25	21.45	21.45	21.45			21.58	21.57		
2.0	34.93	34.96	34.94	33.49	33.36	35.23	35.20	35.64	35.68
2.9	52.52	52.60	52.57			53.29	53.13		
3.8	73.28	73.51	73.44	73.76	73.36	75.15	74.64	77.32	76.53
4.4	91.32	91.75	91.58			94.42	95.46		
4.75	106.38	106.98	106.78	108.94	107.85	110.76	109.34	117.35	114.12
4.9	116.34	117.01	116.78			121.37	119.73		
4.95	121.32	121.98	121.73	124.32	123.04	126.44	124.74	134.41	130.49
4.975	124.84	125.50	125.25	127.68	126.37	130.02	128.29	137.76	133.77

$$f_N^2 = \frac{f_P^2}{2} \left\{ 1 + \cos \left[\frac{3\pi (Z_M - Z)}{4Y} \right] \right\}$$

with $f_P = 5$ mc,

$Z_M = 133.3$ km,

$Y = 100$ km.

The virtual heights were taken from a table prepared by Becker (1960), and these were then reduced by the preceding parabolic method as well as by the Budden method. The first virtual height is zero, corresponding to the bottom of the layer. The improvement in accuracy is readily seen.

With real ionograms, however, virtual heights are not visible below some minimum frequency, f_{min}. It is obvious that any number of h'(f) curves could be drawn below f_{min}, each giving a different electron density distribution above as well as below f_{min}. A common assumption is that of a flat base, with all virtual heights below f_{min} equal to the value at f_{min}. The resulting profile is flat below f_{min} and everywhere higher than the original layer. During the day, the flat base assumption is relatively good for the F region, but at night serious errors can result. Titheridge (1961) has published empirical correction formulas for these night time profiles.

Special low frequency ionograms (O'Brien and Ross, 1958); VanMeter, 1950; Sulzer and Underhill, 1949; Hardy, 1963) indicate

that the virtual heights near 75 kc are relatively constant at 95 ± 15 km both diurnally and seasonally. Thus, the first parabola can be computed by putting $Z_1 = 95$ km and using, in addition, the first two scaled virtual heights. The reduction then proceeds in the normal step-by-step fashion. Examples of these last two techniques are presented after the following section.

3. JOINT ORDINARY AND EXTRAORDINARY MODE ANALYSIS WITH LEAST SQUARES

One of the most important problems of reducing bottom-side ionograms to electron density profiles is the fact that echoes are not seen down to zero plasma frequency. As mentioned earlier, with a single magneto-ionic mode, and in the absence of other information, there is no unique electron density profile.

Storey (1960) suggested that this problem could be resolved by simultaneous solution of the equations for the ordinary and extraordinary modes. Whether a unique solution exists, in general, has not yet been answered definitely (Brown, 1964). However, with the restriction of any particular shape for each segment, including the first, a unique solution can be found. Such a profile cannot be expected to produce virtual heights agreeing exactly with the scaled values. Consequently, we seek a profile which minimizes, with respect to the lamination parameters, the sum of the squares of the differences between the observed virtual heights and those produced by the profile. It should be noted that this calculated profile is not necessarily the best fit to the actual ionosphere . In fact, some entirely unreasonable distributions have produced better agreement of virtual heights than others which more closely approximate the model used. An important feature of the least squares method is that additional data in excess of the minimum needed for a

solution can be utilized to reduce the effect of scaling errors and to improve the stability of the solutions.

Assume that the ordinary mode virtual heights have been scaled at arbitrary frequencies f_2 through f_M ($f_1 = 0$). These frequencies are then used to divide the true height profile into parabolic segments so that the size of each segment is easily controlled. In addition to the M-1 scaled ordinary mode points, suppose that N extraordinary mode virtual heights have been scaled at arbitrary frequencies f_{X1} through f_{XN}. Because the first parabolic segment, which extends from $f_N = 0$ to $f_N = f_2$, has two extra unknowns, at least two extraordinary samples are required; in practice about four points are scaled.

Then equation (4) is written as

$$
\begin{aligned}
h'_o(f_2) &= a_1 D_{21} + b_1 D_{22} + 0 + \cdots + Z_1 D_{2,M+1} \\
h'_o(f) &= a_1 D_{31} + b_1 D_{32} + b_2 D_{33} + 0 + \cdots + Z_1 D_{3,M+1} \\
&\vdots \\
h'_o(f_M) &= a_1 D_{M,1} + b_1 D_{M,2} + \cdots + b_{M-1} D_{M,M} + Z_1 D_{M,M+1} \qquad (5) \\
h'_x(fx_1) &= a_1 D_{M+1,1} + b_1 D_{M+1,2} + \cdots + b_{j-1} D_{M+1,j} + 0 + \cdots + Z_1 D_{M+1,M+1} \\
h'_x(fx_N) &= a_1 D_{M+N,1} + b_1 D_{M+N,2} + \cdots + b_{k-1} D_{M+N,k} + 0 + \cdots + Z_1 D_{M+N,M+1}.
\end{aligned}
$$

In the above, (2) has been employed to relate a_2 through

a_{M-1} to a_1 and the b's. The coefficients D_{jk} are constants and are computed as follows:

$$D_{j,\,M+1} = 1, \quad j = 2,\ M+N$$

$$D_{j,1} = \sum_{k=1}^{j-1} \int_{f_{N_k}}^{f_{N_{k+1}}} \mu'(f_j)\, df_N, \qquad k = 2,\ M+N;$$

$$D_{jk} = \int_{f_{N_{j-1}}}^{f_{N_j}} (f_N - f_{N_{j-1}})\, \mu'(f_j) df_N + 2(f_{N_k} - f_{N_{k-1}}) \sum_{f_{N_1}}^{j-1} \int_{f_{N_1}}^{f_{N_{1+1}}} \mu'(f_j)\, df_N,$$

$$j = 2,\ M+N;\ k = 1,\ M+N-1;$$

$$D_{jj} = 2 \int_{f_{N_{j-1}}}^{f_{N_j}} (f_N - f_{N_{j-1}})\, \mu'(f_j)\, df_N, \qquad j > 1.$$

For the extraordinary mode, the highest value of f_N is that corresponding to reflection, and the appropriate extraordinary wave frequency is used.

To simplify the notation, let the variables a, b, and Z be represented by X so that $a_1 = X_1$, $b_j = X_{j+1}$, and $Z_1 = X_{M+1}$. In

matrix notation, equation (5) is

$$\underline{\underline{D}}\ \underline{\underline{X}} = \underline{\underline{h'}}\ . \qquad (6)$$

There are M+1 unknowns with M+N-1 linearly independent equations. Lanczos (1956) states that the least squares solution of (6) is the solution of

$$\underline{\underline{D}}^t\ \underline{\underline{D}}\ \underline{\underline{X}} = \underline{\underline{D}}^t\ \underline{\underline{h'}} \qquad (7)$$

where $\underline{\underline{D}}^t$ is the transpose of $\underline{\underline{D}}$. This is proved in Appendix 2. Now $\underline{\underline{D}}^t\ \underline{\underline{D}}$ is an M+1 by M+1 symmetric array, and $\underline{\underline{D}}^t\underline{\underline{h'}}$ is an M+1 column thus producing M+1 equations in M+1 unknowns. Equation (7) is solved for each X by Gaussian elimination rather than by matrix inversion to reduce computational errors. The remaining a's are calculated from (3) and the true heights are then given by (4).

3.1 MODEL COMPUTATIONS

The techniques discussed in the previous sections were tested on typical day and nighttime model profiles as shown in Figure 2. The computed ionograms are shown in Figures 3 and 4, where the scaled points are shown by dots. In order to provide a realistic test, all scaled virtual heights were rounded to the nearest 5 km., since such scaling accuracy is easy to achieve in practice, and is

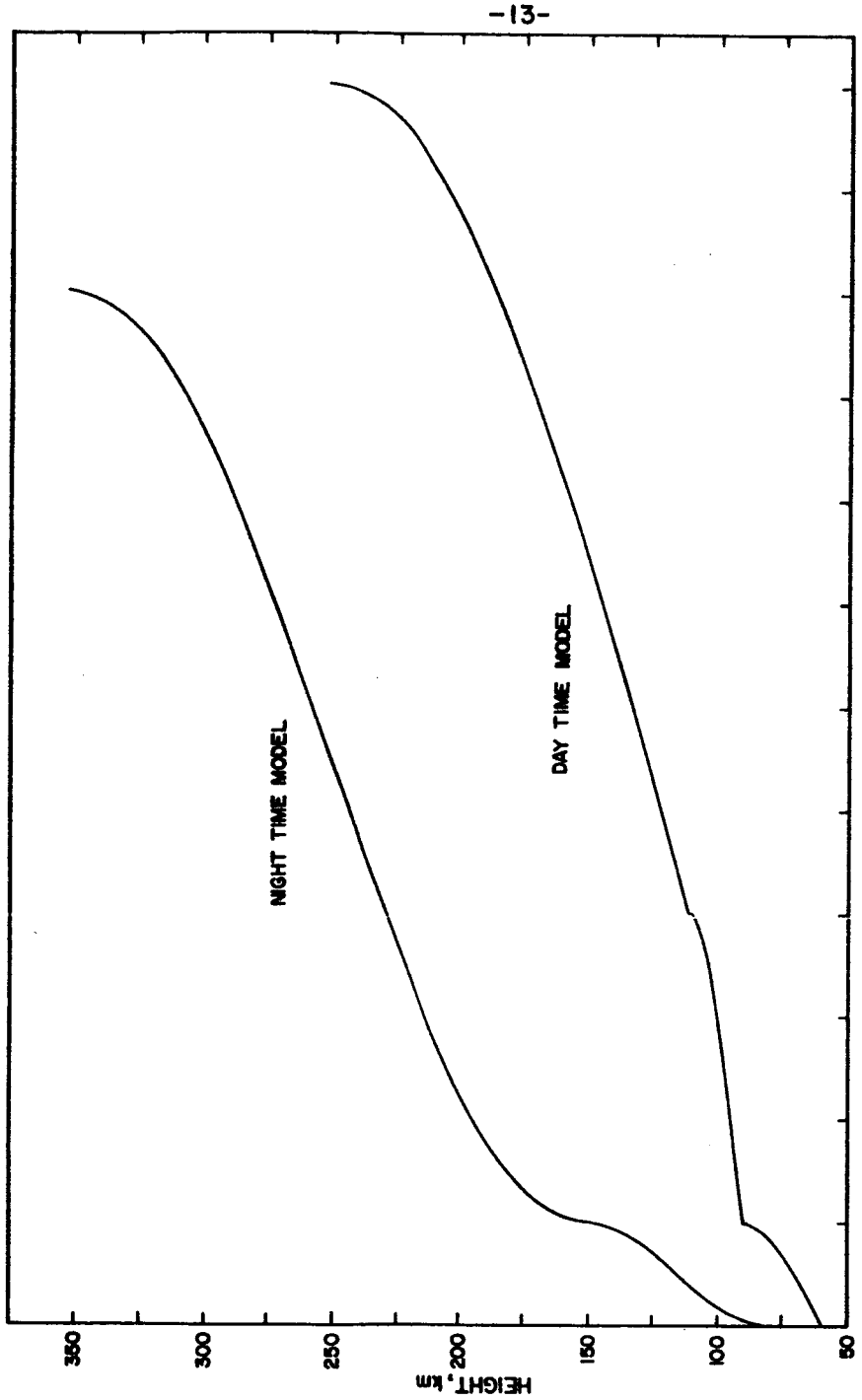

BOTTOMSIDE MODELS USED IN TESTS

FIGURE 2

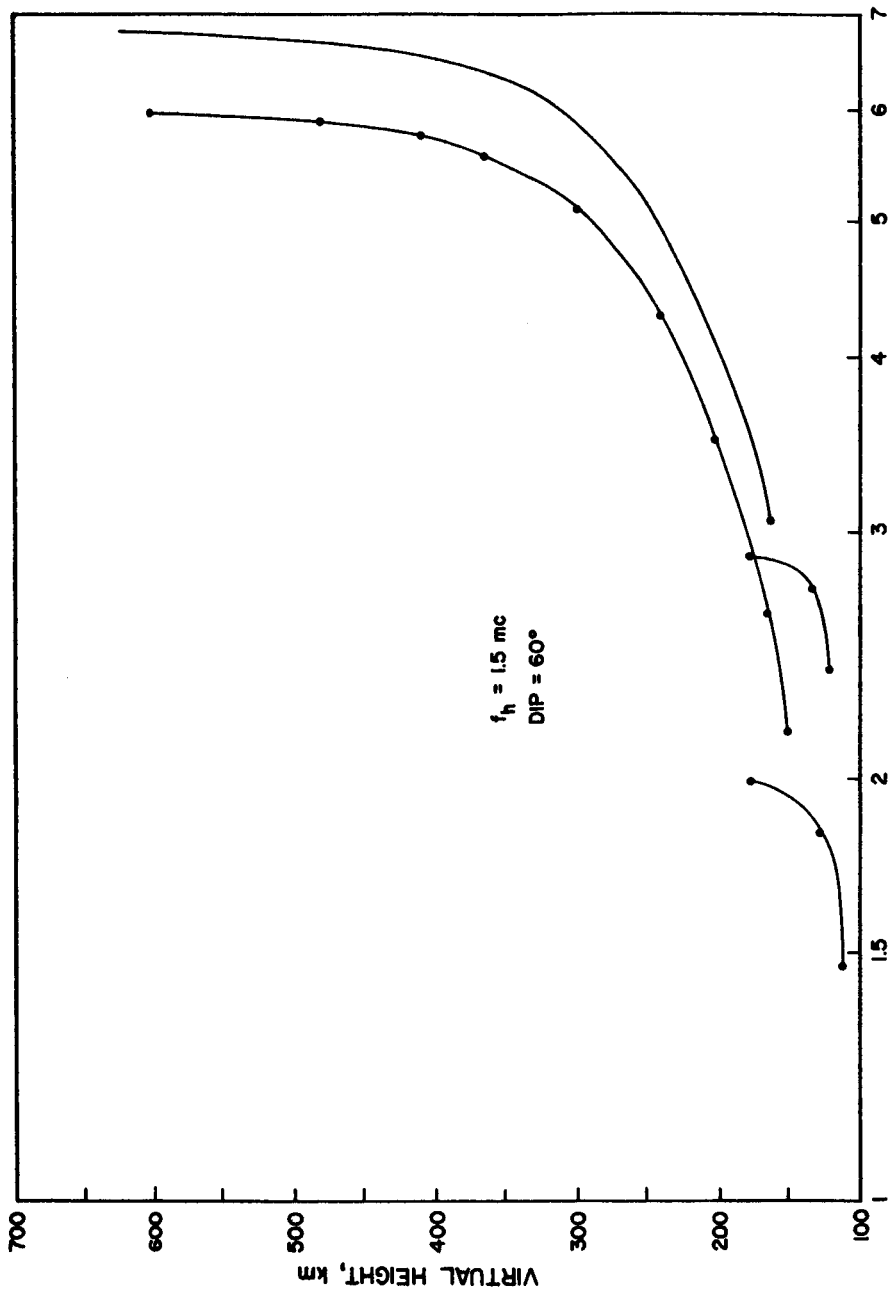

VIRTUAL HEIGHTS FROM DAYTIME MODEL. DOTS INDICATE SCALED POINTS

FIGURE 3

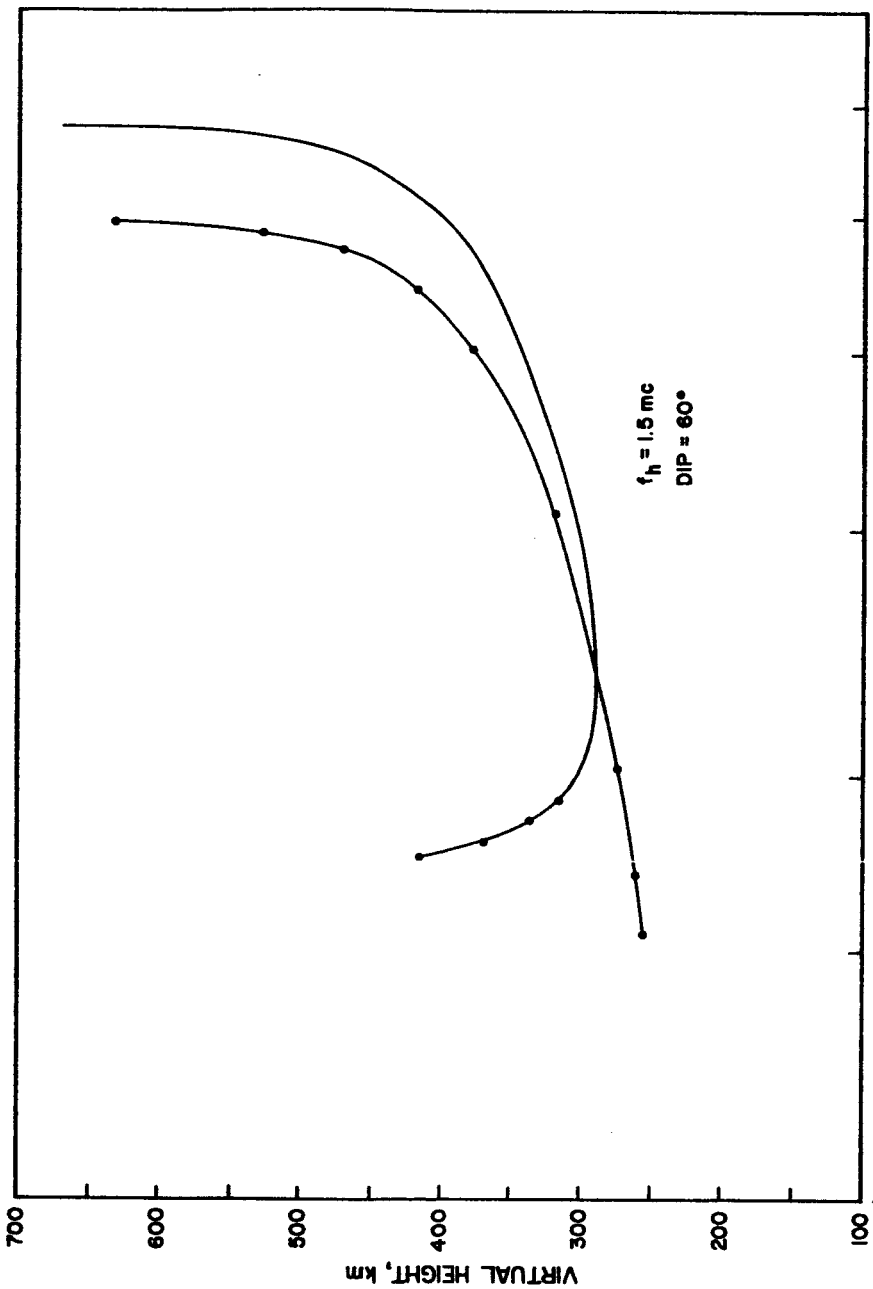

VIRTUAL HEIGHTS FROM NIGHT TIME MODEL. DOTS INDICATE SCALED POINTS

FIGURE 4

in fact, often exceeded.

The results from the daytime model are shown in Table 2, where the errors are indicated. It is seen that the flat base assumption is the worst, and that there is no significant difference between the other results.

Computed profiles for the nighttime model are shown in Figure 5. Here, the differences between alternative methods of compensating for underlying ionization are more pronounced, due to the increased thickness of the lower portion of the profile. The first base assumption leads to large errors; as is well known.

Table 2

True Height Errors for Model in Figure 3

Bottomside Daytime Plasma Freq(mc)	Model Height (km)	Flat Base	(Calculated-Model) Heights, km: Single Mode With Z_1 = 80km	95km	110km	Least Squares Without h'_o(75kc)	Least Squares With h'_o (75kc) = 80km	95km	110km
1.475	100	15.0	-0.5	3.9	8.2	3.9	-0.8	2.0	4.8
1.835	105	16.6	+0.2	3.4	6.7	3.3	-0.5	2.1	4.7
2.000	110	12.1	1.7	4.8	7.7	4.6	+1.3	3.7	6.0
2.180	115	12.5	3.3	5.9	3.7	5.7	2.8	4.9	6.9
2.625	125	7.7	0.3	2.4	4.6	2.4	0.0	1.5	3.1
3.500	145	6.7	1.5	3.0	4.6	2.9	1.3	2.4	3.6
4.460	170	5.4	1.4	2.5	3.8	2.5	1.2	2.1	3.0
5.235	195	5.3	1.9	2.9	3.9	2.9	1.8	2.6	3.3
5.760	220	6.4	3.4	4.2	5.2	4.2	3.2	3.9	4.6
5.900	230	7.3	4.3	5.2	6.1	5.1	4.2	4.9	5.5
5.935	235	6.2	3.3	4.1	5.0	4.1	3.2	3.8	4.5
5.970	240	6.5	3.6	4.5	5.3	4.4	3.5	4.1	4.8

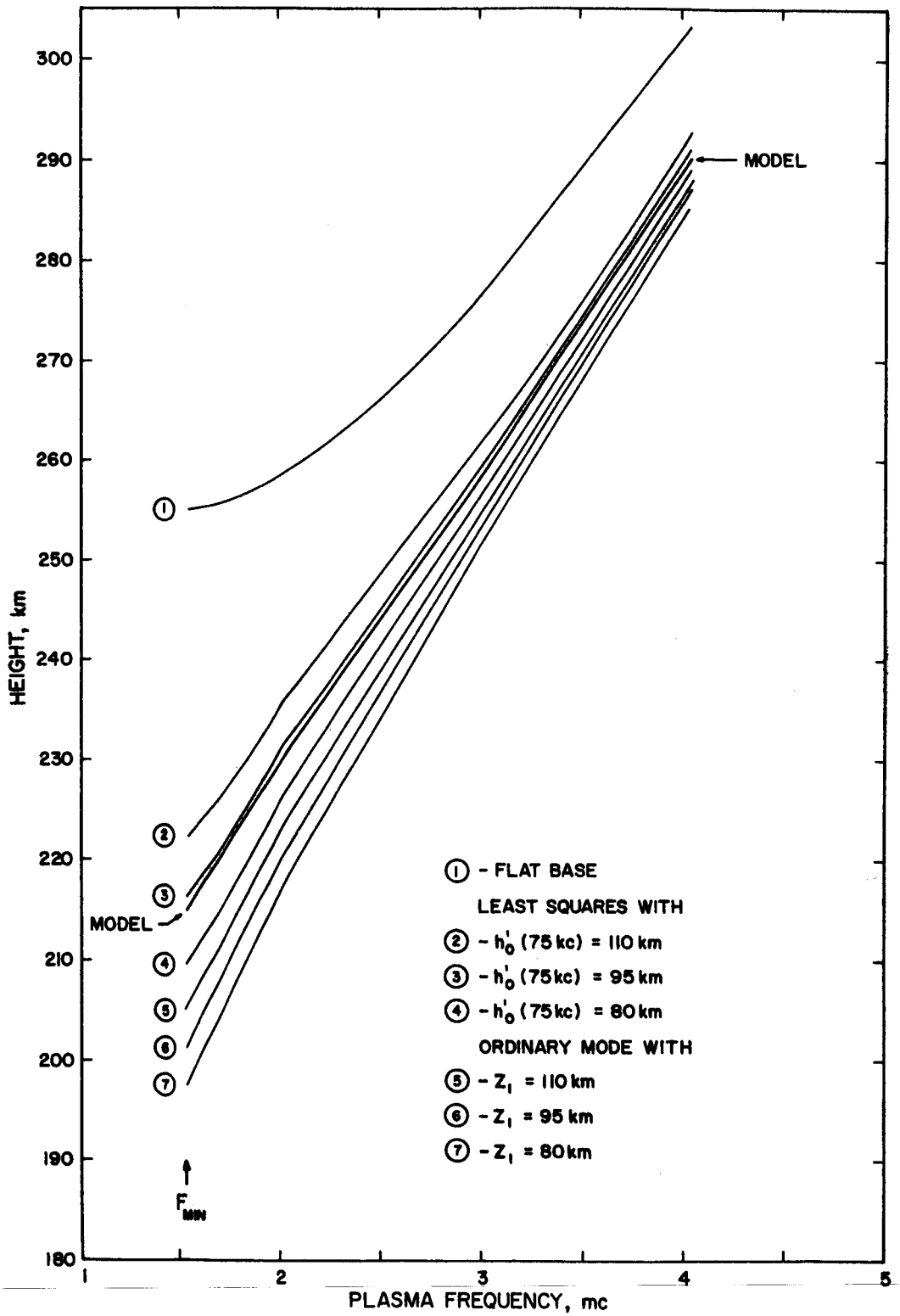

ELECTRON DENSITY PROFILES CALCULATED FOR THE NIGHT TIME MODEL

FIGURE 5

The best solution was obtained with the least squares technique and a known virtual height at 75 kc/s. It is to be noted, from curves 2, 3, and 4, that errors of 15 km. in this low frequency virtual height result in much smaller errors in the F region profile. Since average values for day and night conditions are certainly known to this accuracy, it is suggested that the inclusion of such a low frequency average virtual height provides a simple method of compensating for underlying ionization.

3.2 SOME ACTUAL PROFILES

Figures 6 and 7 show profiles computed from actual ionograms taken at Fort Belvoir at 1300 EST on December 23, 1957, and at 0001 EST on the same day; respectively.

A least squares analysis of the former could not be performed because the extraordinary trace was not observed below 5 mc. At this high a frequency the influence of the region below f_{min} in the extraordinary trace is too small for this mode to be of use. Differences between the flat base and Z_1 = 95 km single mode solutions of the daytime ionogram are about 17 km at f_{min}, but at night this difference increased to 50 km. The actual nighttime profile is probably near the least squares solutions since it has been seen from the model studies that the single mode solutions at night are somewhat below the true profile. Thus, the correction obtained by least squares joint mode analysis over the flat base analysis is about 30 km.

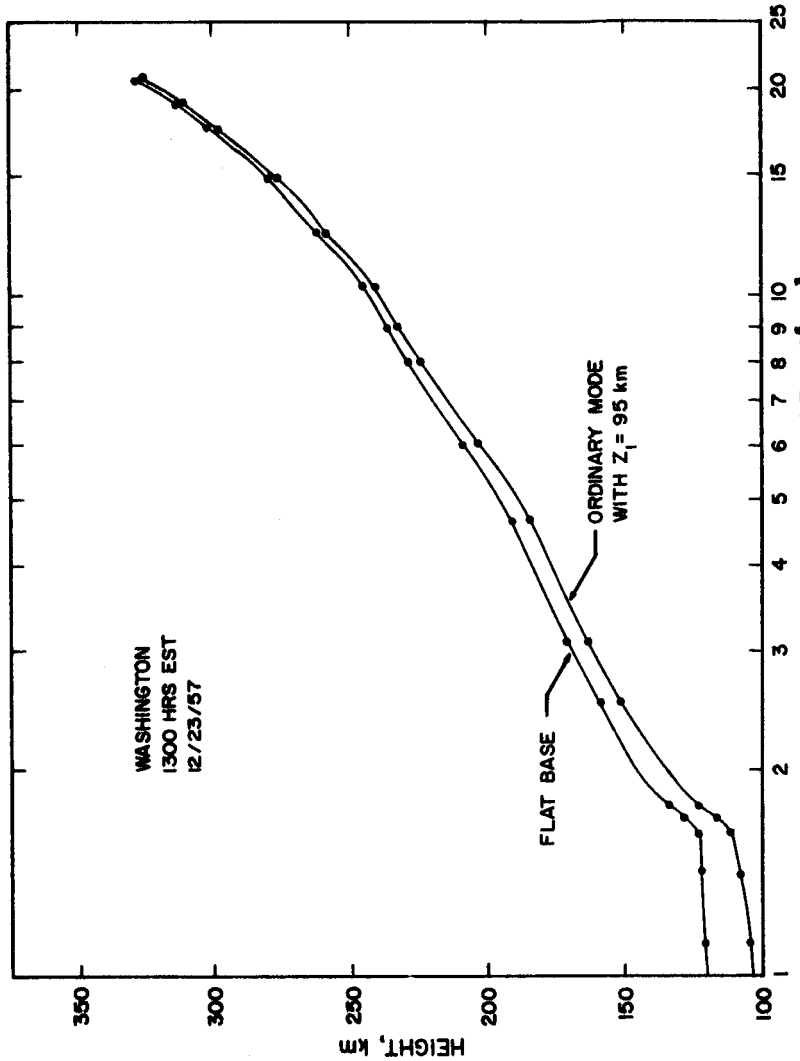

TRUE HEIGHT COMPUTED FROM AN ACTUAL IONOGRAM.
DOTS INDICATE THE COMPUTED POINTS. A LEAST SQUARES
ANALYSIS WAS NOT POSSIBLE BECAUSE THE EXTRAORDINARY
MODE WAS NOT OBSERVED TO A SUFFICIENTLY LOW FREQUENCY.

FIGURE 6

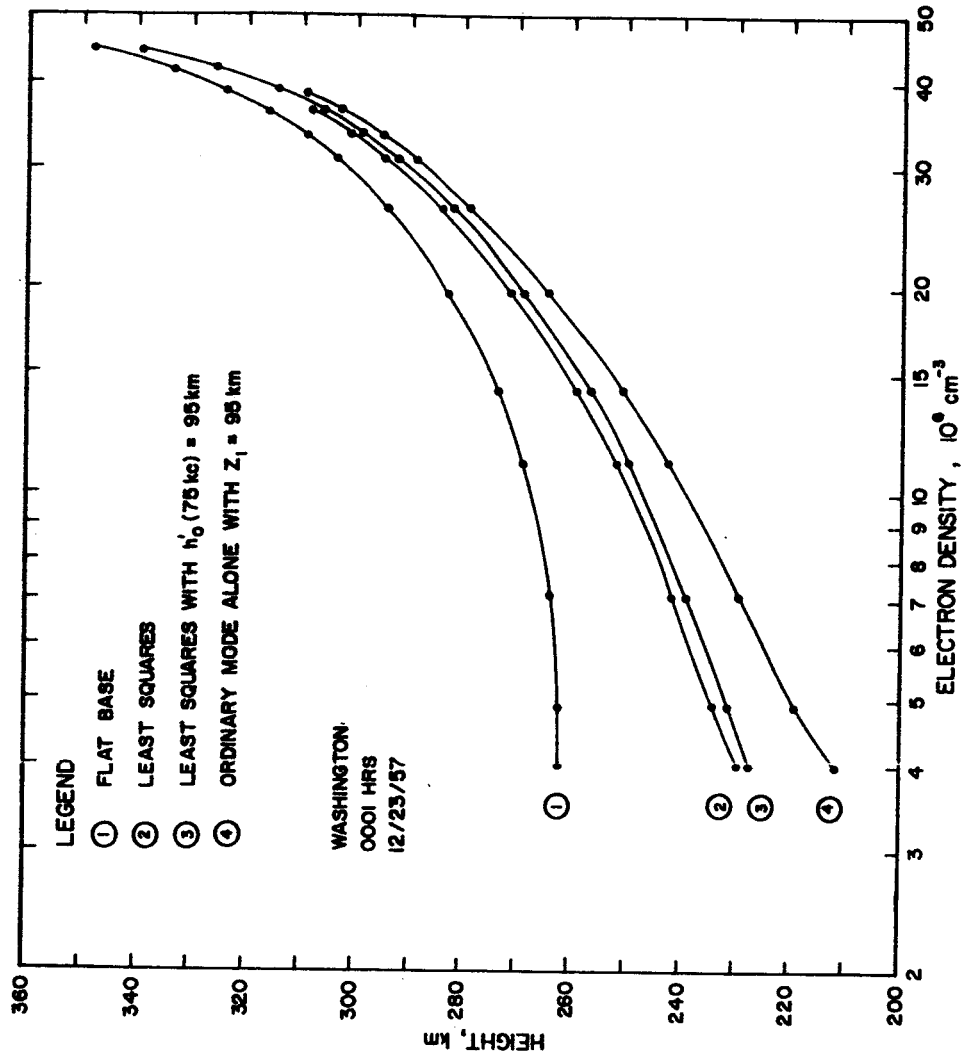

RESULTS FROM A NIGHT TIME IONOGRAM. DOTS INDICATE CALCULATED POINTS

FIGURE 7

A minimum of two extraordinary virtual heights are required by the least squares program, and four were used in these computations. With only two samples, the effects of rounding errors in the data become more pronounced, but with four samples these errors have little effect. It has been observed that if these ordinary mode samples whose frequency is above the highest extraordinary mode plasma frequency of reflection are removed, then the remaining profile remains unchanged. Thus, addition of high frequency ordinary mode samples does not affect the lower portion of the profile. If high frequency extraordinary samples are also included the lower portion of the profile changes in order to minimize all of the residuals. High frequency extraordinary mode samples have a detrimental effect on the profile as a whole so that only four samples are usually taken near the beginning of the extraordinary trace on the ionogram.

4. THE TOPSIDE

Regular soundings have recently been made by the Alouette satellite from 1000 km down to the F2 electron peak (Chapman, 1963). These are analogous to the bottomside soundings but differ from them in several important details.

The sounder is immersed in the ionosphere, and echoes are not seen until the plasma frequency of reflection exceeds the

plasma frequency around the satellite (Fitzenreiter and Blumle, 1964). The extraordinary mode virtual height, measured downward from the satellite, is usually seen to zero range, so that there is no low frequency cut-off problem. Ordinary mode echoes, however, are seldom seen down to zero range (King et al., 1963), and for this reason only the extraordinary mode is usually reduced.

It is found that the profile, except near the F2 peak, can be approximately described over fairly large ranges by Z proportional to log f_N. We therefore chose segments of the form

$$Z = Z_j + a_j(\log f_N - \log f_{N_j}) + b_j (\log f_N - \log f_{N_j})^2,$$

$$\text{for} \quad f_{N_j} \leq f_N \leq f_{N_{j+1}}$$

In this section, Z is defined as the distance <u>below</u> the satellite. Since this equation can be made to represent the profile quite well over rather large height ranges, only a small number of segments need be used to obtain high accuracy. Furthermore, difficulties connected with scaling topside ionograms at low frequencies, where h'(f) increases rapidly, can be avoided because the curvature of parabolic segments allows more widely spaced samples to be taken. Other workers have chosen linear laminations in log N (Fitzenreiter and Blumle, 1964),

parabolic laminations in log f_N^2 (Paul and Wright, 1963), and polynomials in f_N (Knecht et al., 1962; Thomas and Long, 1963; and Thomas and Westover, 1963).

An important complication arises from the fact that the variation of gyrofrequency, f_h, with altitude cannot be ignored on the topside since it varies by about 30% between 1000 and 250 km. For the extraordinary ray, this variation enters the computations in two places; in the plasma frequency of reflection, $f_{N_r} = \sqrt{f^2 - f f_h}$, where f_h must be evaluated at the (initially unknown) altitude of reflection, and in the computation for the refractive index. The former effect is the most important, but the second is not negligible and, of course, it is the only effect which would arise if the ordinary ray were used.

Four techniques of gyrofrequency compensation have been developed, the first and fourth by one of us (J.R.D.). Each of these has been applied to the single mode method presented earlier; that is, solving equations of the form

$$h'(f_k) = \sum_{j}^{k=1} \left[a_j \int_{\log f_{N_j}}^{\log f_{N_{j+1}}} \mu' \, d \log f_N + 2b_j \int_{\log F_{N_j}}^{\log f_{N_{j+1}}} (\log f_N - \log f_{N_j}) \, \mu' d \log f_N \right]. \tag{8}$$

Technique 1. Post Reduction

The gyrofrequency is held constant and equal to its value, f_{h_s}, at the satellite throughout the computation of the entire profile. This means that μ'_x is too small, and that each plasma frequency of reflection, f_{N_j}, is too large. These two errors tend to cancel in the evaluation of the integrals of μ'_x so that the true heights, Z_j, are fairly accurate. At each height Z_j, f_h is evaluated by either an inverse cube law or a polynomial expansion for the magnetic field. A new value for each f_{N_j} is then found from

$$f_{N_j} = \sqrt{f_j^2 - f_j f_h(Z_j)} \tag{9}$$

Thus, the profile is shifted to lower values of electron density at each height. This is the simplest of the four techniques and derives its name from the fact that no compensation is applied until all the true heights have been found.

Technique 2. Step-by-step

The gyrofrequency is held constant only over a lamination. For each lamination it is computed at the height of the beginning (or top) of the lamination and is then used in calculating both μ'_x and f_{N_r}. Thus, f_h is periodically reevaluated and increases in steps going down the profile. Here again μ'_x is too low and f_{N_r} is too high because f_N corresponds to an altitude at the

beginning of a lamination rather than at a lower altitude. The errors in μ'_x and f_{N_r} do tend to cancel somewhat, but the integrals of μ' are too large. Therefore, the profile will be too great an altitude above the ground and the densities at these heights will be a little too large.

Technique 3. Step-by step with Post Reduction

The preceding methods are combined so that f_h increases in steps and f_{N_r} is reevaluated at each height of reflection. To illustrate the technique, consider the first lamination. Both f_{N_r} and the integrals of μ'_x are calculated with $f_h = f_{h_s}$, and the following parabolic segment is found:

$$Z = Z_1 + a_1(\log f_N - \log f_{N_1}) + b_1 (\log f_N - \log f_{N_1})^2 \qquad (10)$$

where $Z_1 = 0$, and f_{N_1} is the plasma frequency at the satellite. The height, Z_2, at the bottom of the segment is given by equation (10) when

$$f_N = f_{N_2} = \sqrt{f_2^2 - f_2 f_{h_s}} \, . \qquad (11)$$

In the section on technique 1 it was pointed out that the errors in f_{N_r} and μ'_x arising from a constant f_h tend to cancel in the integrals of μ'_x so that the height of reflection, Z_2, is nearly correct. The compensation procedure is then to

recompute f_{N_2} by equation (10) with f_{h_s} replaced by f_h at Z_2. This new and smaller f_{N_2}, however, is not consistent with equation (10) at height Z_2. We seek values for f_{N_2} which satisfies equation (10) and

$$f_{N_2} = \sqrt{f_2^2 - f_2 f_h (Z)} \tag{12}$$

where $f_h (Z)$ is the gyrofrequency at any height Z; $f_h (Z=0) = f_{h_s}$. Equation (10) and (12) are plotted together in Figure 8; $f_h(Z)$ was assumed to obey the inverse cube law

$$f_h (Z) = f_{h_s} \left(\frac{R+H_s}{R+H_s-Z} \right)^3 \tag{13}$$

where R is the mean earth radius, and H_s is the altitude of the satellite. The desired value for F_{N_2} is found from the intersection of these curves. The height at this intersection becomes the new height of reflection, Z_2, and is less (nearer the satellite) than originally computed. Since Z_2 was nearly correct originally, this new value will be too small. This completes the evaluation of the first lamination.

Evaluation of the second lamination procedes in the same manner, except that below Z_2 the gyrofrequency is assumed to be the value at Z_2.

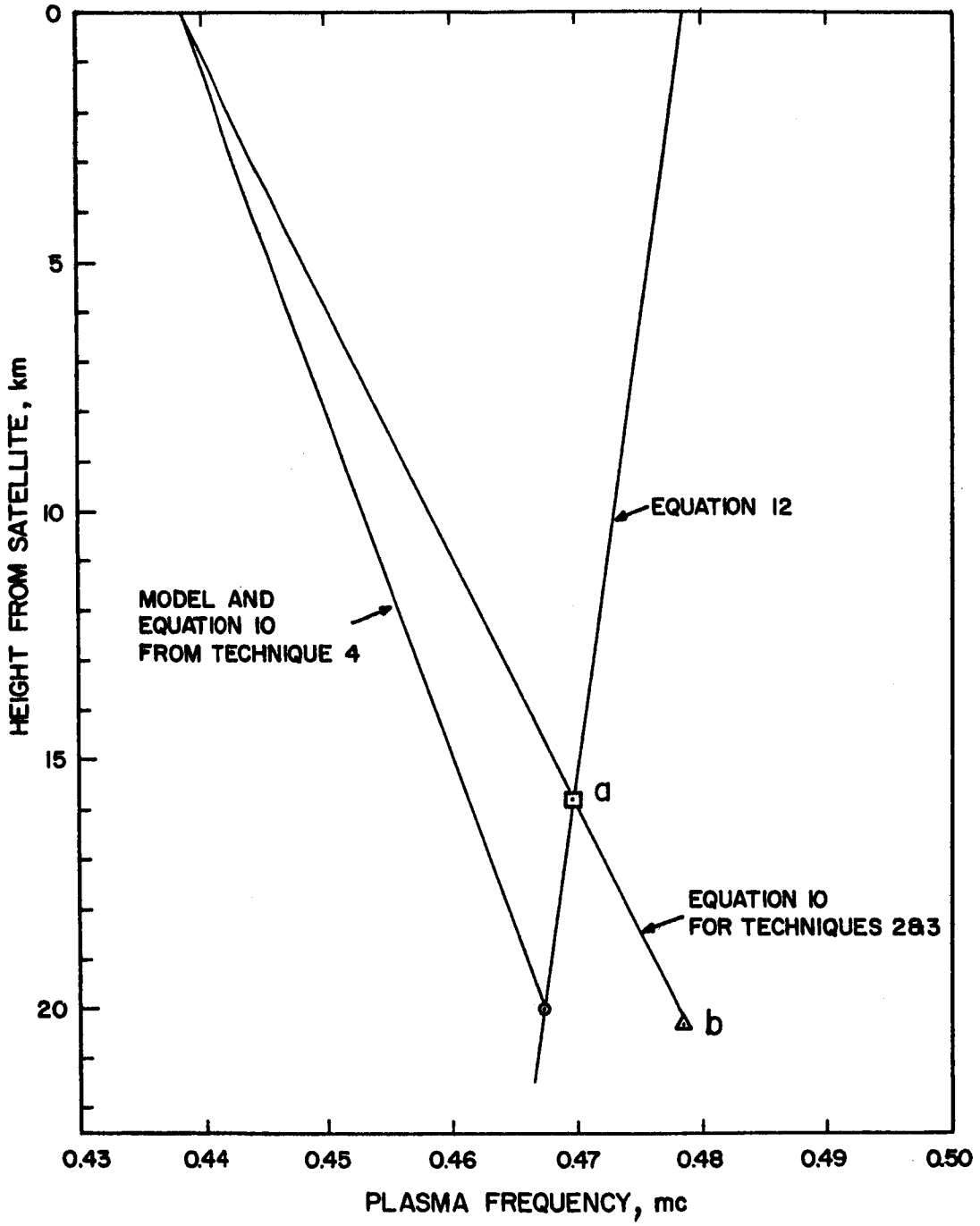

SOLUTION FOR THE EXTRAORDINARY MODE PLASMA FREQUENCY OF REFLECTION. POINT a IS THE SOLUTION BY TECHNIQUE 3 AND POINT b IS THAT BY TECHNIQUE 2. THE MODEL AND SOLUTION BY TECHNIQUE 4 ARE SHOWN FOR COMPARISON.

FIGURE 8

Technique 4. Iterative

The ideal solution to the compensation problem would be to compute integrals of μ' and the plasma frequencies of reflection with a continuously varying gyrofrequency. The first lamination will be considered separately from the others because it is treated somewhat differently. Consider the first lamination. We wish to solve the equations

$$\left.\begin{aligned} h'_x(f_1) &= 0 \\ h'_x(f_2) &= a_1 \int_{\log f_{N_1}}^{\log f_{N_2}} \mu'_x(f_2, f_N, f_h, \phi)\, d\log f_N + 2b_1 \int_{\log f_{N_1}}^{\log f_{N_2}} (\log f_N / f_{N_1})\, \mu'_x\, d\log f_N \\ h'_x(f_3) &= a_1 \int_{\log f_{N_1}}^{\log f_{N_2}} \mu'_x(f_3, f_N, f_h, \phi)\, d\log f_N + 2b_1 \int_{\log f_{N_1}}^{\log f_{N_3}} (\log f_N / f_{N_1})\, \mu'_x\, d\log f_N \end{aligned}\right\} \quad (14)$$

for the constants a_1 and b_1 with the gyrofrequency varying with height. Here ϕ is the angle between the wave normal (vertical) and the earth's magnetic field. It should be noted that, although the parabolic segment extends over two laminations, only the first part will be used in the final profile.

Since we wish to include a varying f_h, it must be expressed as a function of f_N in order to be included in the integrals. Initially,

there is no relation for f_h (f_N), and f_h is assumed to be a constant equal to f_{h_s}. The plasma frequencies of reflection, f_{N_2} and f_{N_3}, are computed from

$$f_{N_j} = \sqrt{f_j^2 - f_j f_{h_s}} \quad , \quad j = 1, 2, 3 \ .$$

with f_{N_1} equal to the plasma frequency at the satellite. Equation (14) is now solved for a_1 and b_1 to give the parabolic segment

$$Z = a_1 (\log f_N - \log f_{N_1}) + b_1 (\log f_N - \log f_{N_1}),$$

$$f_{N_1} \leq f_N \leq f_{N_3} \ . \qquad (15)$$

Equation (15) together with an expression for $f_h(Z)$, such as the inverse cube law

$$f_h(Z) = f_{h_s} \left(\frac{R+H_s}{R+H_s - Z} \right)^3 \quad , \qquad (13)$$

provide an initial relationship between f_h and f_N. In the same way as technique 3, new values of f_{N_j} which are consistent with both the profile and the gyrofrequency can be computed by simultaneous solution of equations (15), (13), and

$$f_{N_j} = \sqrt{f_j^2 - f_j f_h (Z)}.$$

Lamination parameters a_1 and b_1 are then recomputed from equation (14) which now includes the new values of f_{N_j} and a variable gyrofrequency given by equations (13) and (15). The new parameters a_1 and b_1 again provide a relationship between f_h and f_N. The process of solving equation (14) with a previous profile linking f_h to f_N is repeated until the profile no longer changes. This is usually four times for the extraordinary and two times for the ordinary mode.

The second and remaining laminations are computed in the following manner. From the boundary conditions of continuous height and slope between parabolic segments we know that

$$a_j = a_{j-1} + 2b_{j-1} (\log f_{N_j} - \log f_{N_{j-1}}), \quad j \geq 2.$$

To improve the convergence of the solution, f_h is initially assumed to be related to f_N by equation (13) and

$$Z = Z_j + a_1 (\log f_N - \log f_{N_j}) \quad , \quad f_{N_j} \leq f_N \leq f_{N_{j+1}} \quad .$$

The iterative process described above is then applied to f_{N_j} and to the integrals over this lamination to give a final answer for b_j; convergence is the same as for the first lamination.

In this way, a continuously varying gyrofrequency can be incorporated into the calculation of the plasma frequencies of reflection and of the integrals of μ'. Computation time is only about twice that for the simplest method.

4.1 MODEL COMPUTATIONS

Each gyrofrequency compensation technique was tested on two Chapman layer models. An inverse cube law for $f_{h(Z)}$ was assumed in computing the virtual heights. The first model, Figure 9, represents a daytime mid-latitude profile. The second Figure 10, is a simplified, nighttime, high latitude profile used to illustrate reduction difficulties when the electron density is low and the gyrofrequency is high.

In addition to the four techniques presented here, results of the linear lamination method described by Fitzenreiter and Blumle (1964) are shown for comparison. In this method, a lamination is computed initially with a constant value of f_h corresponding to the bottom of the previous lamination. The calculation is then repeated with f_{N_K} and μ'_x using the value of f_h at the bottom of the new lamination.

Results for the daytime model are presented in Table III as normalized errors of both density and height. In the case of height, the normalization was made with respect to the distance from the satellite. The errors are almost entirely due to the techniques because the virtual heights were known to two decimal places and the wave frequencies to four places; the same is true for the nighttime model. (Nighttime model profiles are shown in Figure 11.) Profiles from both step-by step techniques are at greater altitudes and smaller densities than the models.

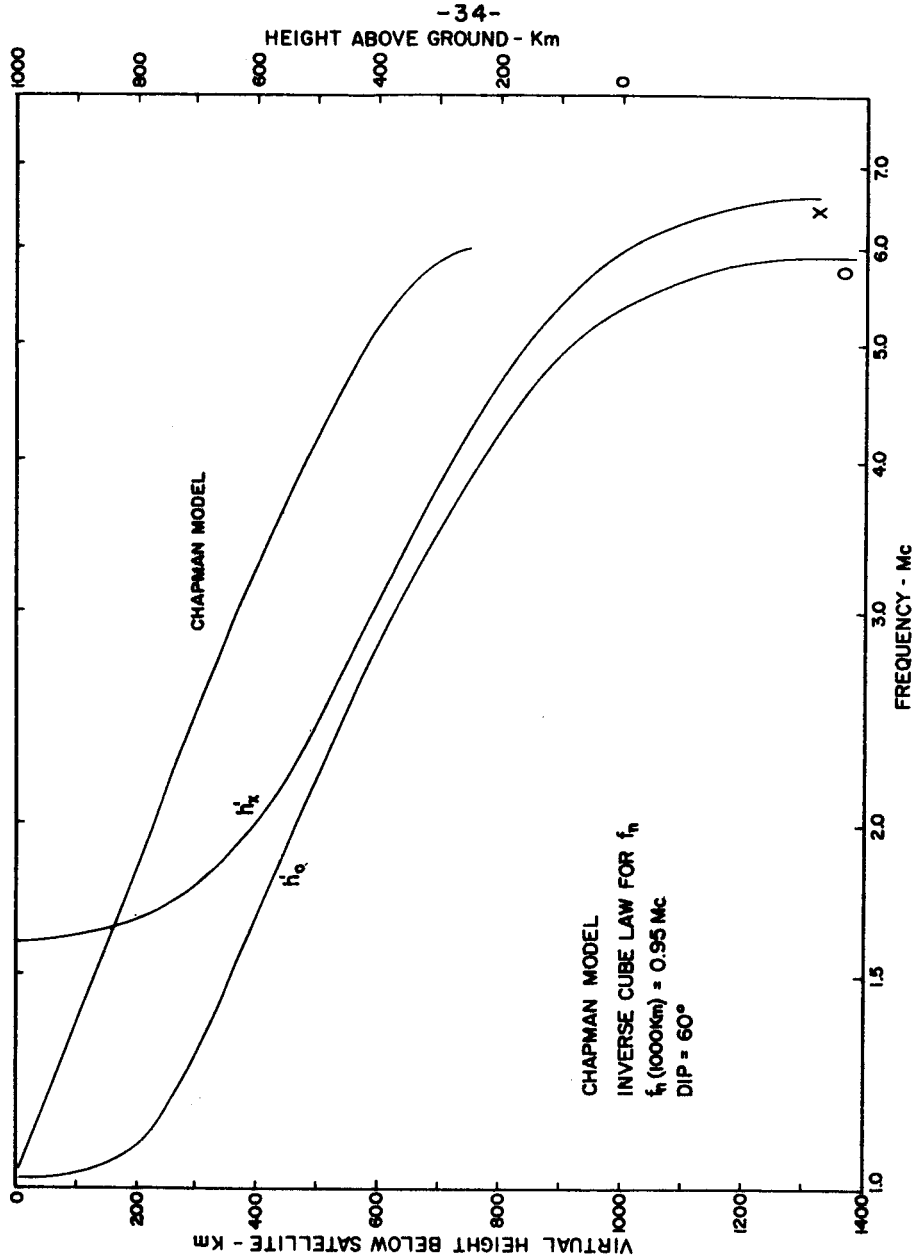

DAYTIME CHAPMAN LAYER MODEL AND CORRESPONDING VIRTUAL HEIGHTS. THE SATELLITE HEIGHT WAS ASSUMED TO BE 1000 Km.

FIGURE 9

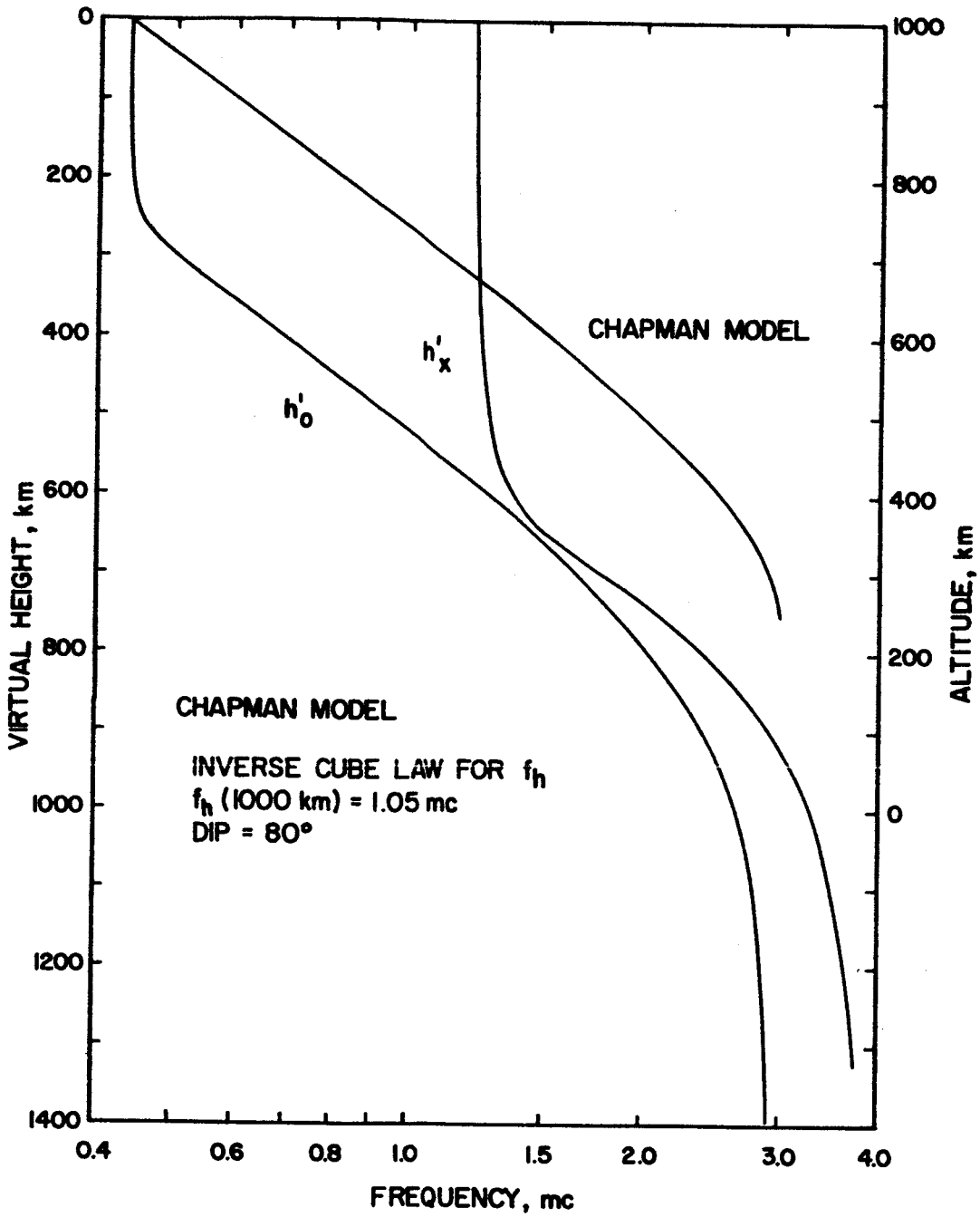

NIGHT TIME CHAPMAN LAYER MODEL AND VIRTUAL HEIGHTS

FIGURE 10

Table III

Relative density and height errors for the daytime Chapman layer model

Daytime Chapman Layer											
Electron Density	Distance Z_M below satellite	Technique 1 Post Reduction		Technique 2 Step-by step		Technique 3 S.S. with P.R.		Technique 4 Iterative		Linear Method	
($10^4 cm^{-3}$)	(km)	ΔN	ΔZ	ΔN	ΔZ	ΔN	ΔZ	ΔN	ΔZ	ΔN	ΔZ
1.2776	0	0	0	0	0	0	0	0	0	0	0
1.3565	10	7.3^{-5}	2.0^{-4}	-5.8^{-3}	2.0^{-4}	-4.4^{-4}	-8.1^{-2}	0	-9.5^{-4}	0	5.6^{-2}
1.5291	30	6.5	2.5^{-3}	-1.1^{-2}	-1.7^{-2}	-1.0^{-3}	-6.8	-6.5^{-5}	-1.4	2.6^{-3}	8.7^{-5}
1.7233	50	0	4.2	-1.0	-2.4	-1.5	-5.5	-5.8	-2.2	4.5	6.7^{-2}
2.3215	100	3.4^{-4}	5.9	-2.1	-9.6^{-3}	-1.8	-4.3	4.3	7.0^{-6}	7.6	4.6^{-3}
4.1872	200	4.1	7.2	-3.1	-9.5	-2.1	-3.3	-2.3	2.5^{-4}	7.2	1.1^{-2}
7.4513	300	4.7	7.1	-2.3	-1.1^{-2}	-1.7	-2.4	-1.3	2.6	9.0	1.6
12.935	400	3.9	6.6	-1.8	-9.1^{-3}	-1.2	-1.7	0	4.3	7.7	1.8
21.459	500	4.7	6.3	-1.4	-7.3	-8.9^{-4}	-1.3	9.3^{-5}	7.7	6.9	2.1
30.382	580	4.6	6.4	-1.0	-6.9	-7.9	-1.1	6.5	1.1	6.4	2.3
36.254	630	4.4	6.3	-6.1^{-3}	-7.5	-7.4	-1.0	8.2	1.2	6.0	2.3
40.464	670	4.9	6.7	-4.9	-7.2	-7.4	-9.7^{-3}	7.4	1.2	6.3	2.3
42.925	700	5.4	7.1	-3.8	-7.6	-7.7	-1.0^{-2}	1.2^{-4}	1.4	7.0	2.3
44.057	710	5.9	7.4	-2.7	-8.5	-8.2	-1.1	1.4	1.6	7.6	2.3
44.434	730	6.1	7.4	-1.7	-9.8	-8.8	-1.1	1.4	1.5	7.0	2.2
44.668	740	6.5^{-4}	7.8^{-3}	-1.9^{-3}	-9.7^{-3}	-9.9^{-4}	-1.2^{-2}	1.6^{-4}	1.8^{-3}	9.1^{-3}	1.9^{-2}

$\Delta N = (N_{CALC} - N_{MODEL})/N_{MODEL}$ $\Delta Z = (Z_{CALC} - Z_{MODEL})/Z_{MODEL}$

With Z measured from satellite

Powers of 10 are indicated by exponents.

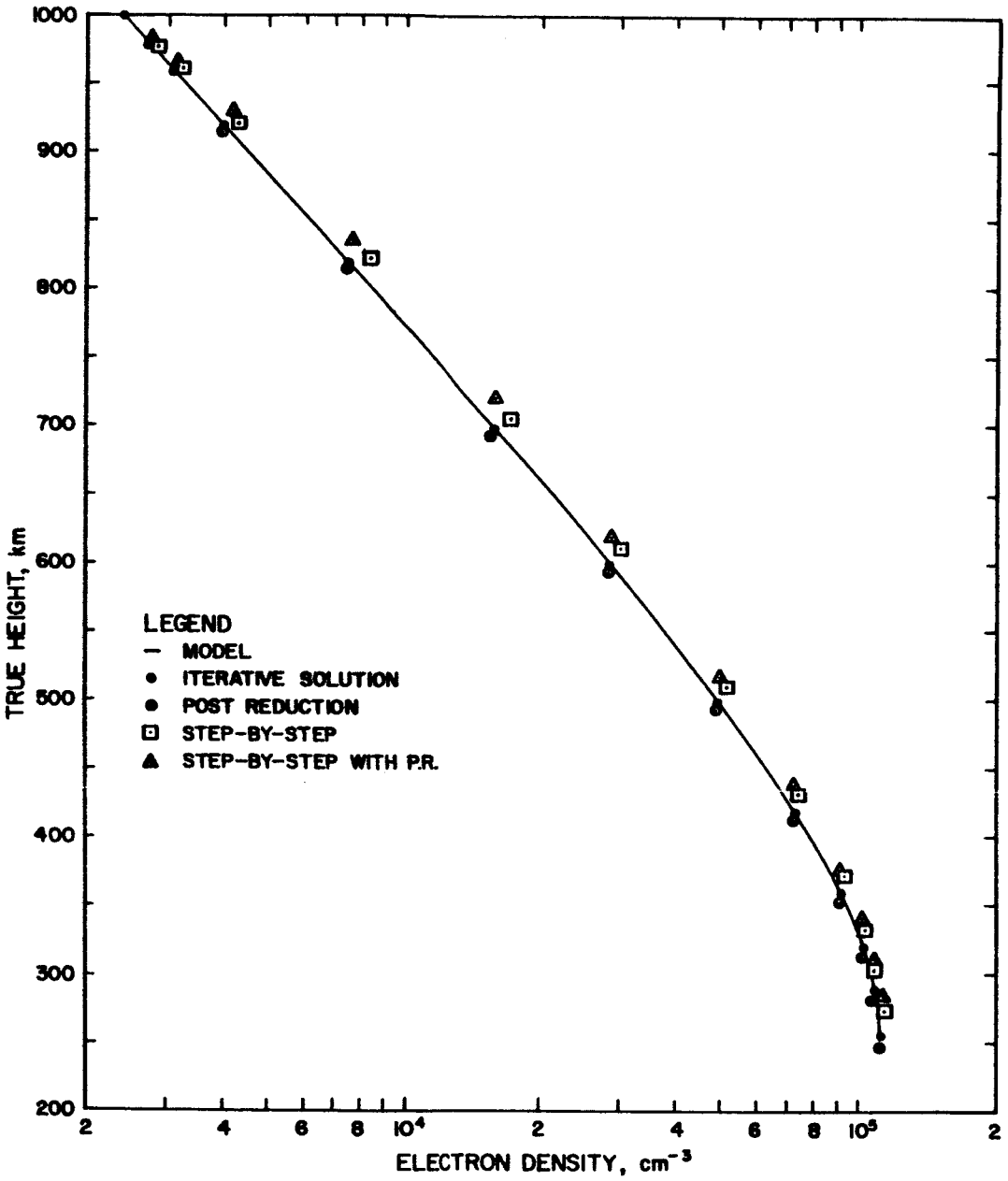

COMPUTED TRUE HEIGHTS FOR THE NIGHT TIME MODEL IN FIG. 10 BY ALL FOUR TECHNIQUES. NOTE THAT BELOW 900 Km. RESULTS OF BOTH STEP-BY-STEP TECHNIQUES LIE ALMOST ALONG A SINGLE SMOOTH CURVE.

FIGURE 11

It is interesting to note that the computed points for both of these techniques, for both models, lie along approximately the same smooth curve. Consequently, the additional correction of f_{N_x} in technique 3 does not improve the basic step-by-step approach. The post reduction technique, however, gave quite good results for both models. This was unexpected because the success of the method depends on cancellation of errors in the integrals of μ'_x. This cancellation was not expected to hold when f_h/f is large (it was 0.84 at the satellite for the nighttime model) because μ'_x is especially sensitive to the variation of f_h when $f_h/f > 0.8$. However, the post reduction correction method is good and better than the step-by-step techniques.

The iterative technique is the most sophisticated and produced the most accurate results. Errors in height and density were very small for both models, about an order of magnitude less than these of the other techniques. The accuracy of the electron density profiles from this technique is limited only by the degree to which parabolic laminations can represent the true profile. Computation time is also short, just double that of the simplest method (post reduction).

The linear lamination method profiles were generally at lower altitudes and smaller densities than the daytime model; near the F2 peak, it was about 16 km too low. However, the nighttime model test shows a different behavior. Near the

satellite, the computed heights were well above the model, but they dropped to a few kilometers below it near the peak. Thus, when fh/f is large, the profile is too high and this error is offset only near the F2 peak where the linear laminations cannot accomodate the model curvature.

The differences between these techniques are most apparent in the computed values of electron density scale height defined by $\frac{1}{H} = -\frac{1}{N}\frac{\partial N}{\partial Z}$. This quantity is important because of its relation to temperatures and ion composition. Computed values of H are shown in Figures 12 and 13. Only the iterative technique agrees almost exactly with the model. In the region near the satellite, the step-by-step techniques show errors in H of up to 30%. Values of H from the post reduction technique are smooth and fairly accurate, while those of the linear method are generally too great. Variations in the computed values of H increase with the ratio fh/f for all techniques except the iterative one.

The electron content of each profile is listed in Table 4 and, as expected, there was little difference between the methods.

From these model studies it has been found that, for accurate topside electron density profiles which can be studied in detail, the iterative method of compensating for fh(Z), coupled with laminations parabolic in log f_N, is well suited and much superior to the other techniques tested.

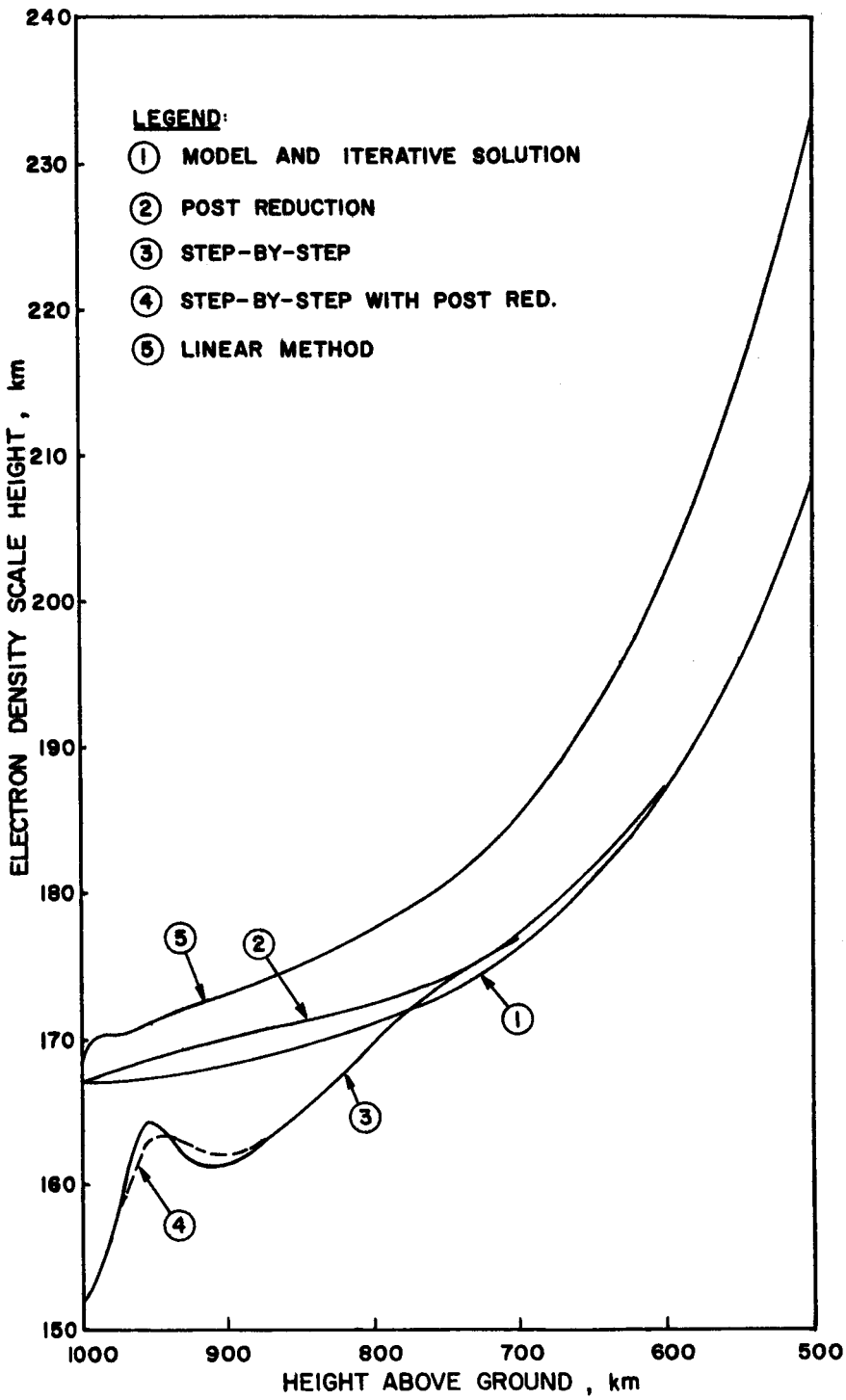

ELECTRON DENSITY SCALE HEIGHTS FOR
THE DAYTIME CHAPMAN LAYER MODEL

FIGURE 12

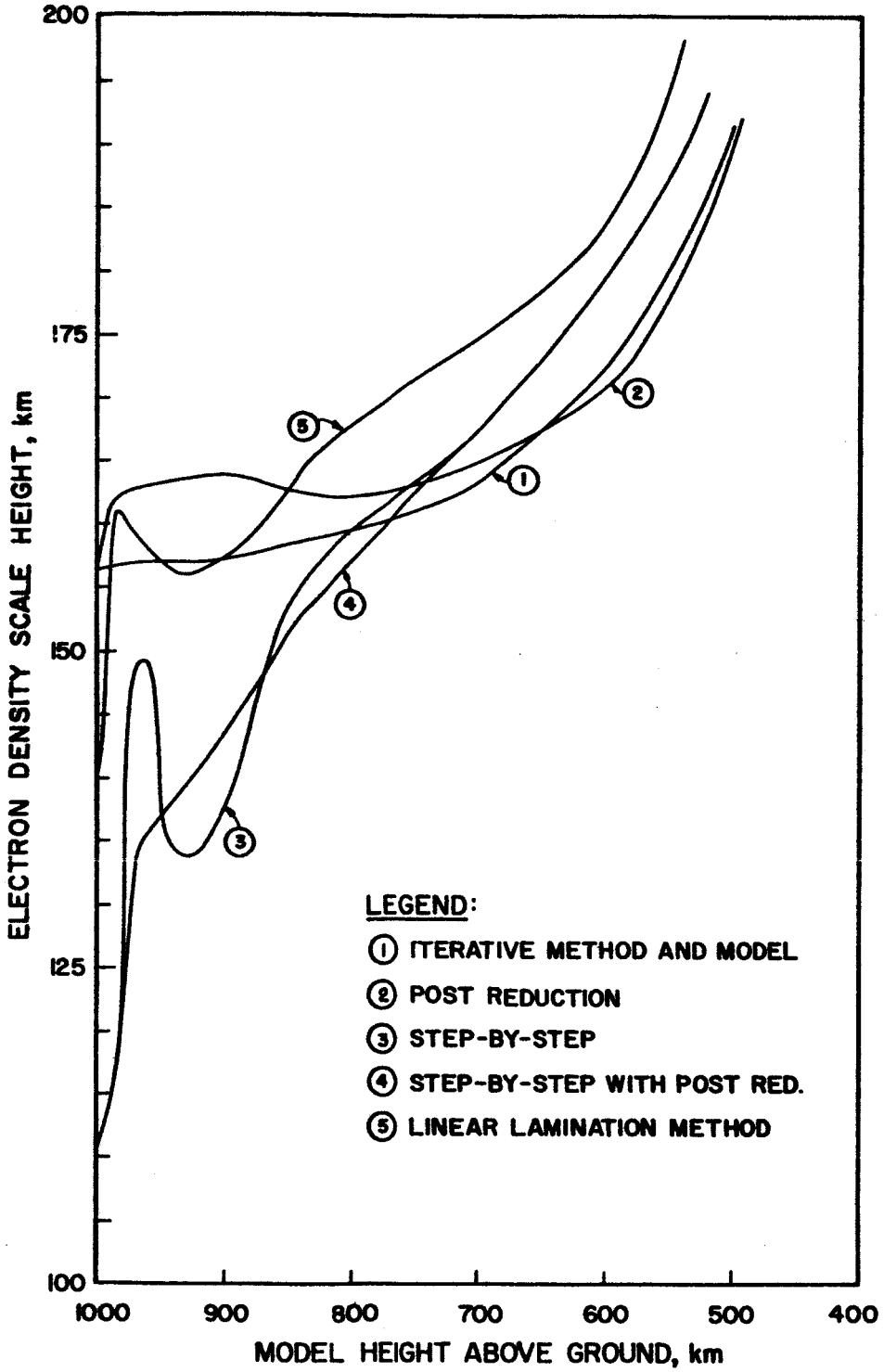

ELECTRON DENSITY SCALE HEIGHTS FOR
THE NIGHT TIME CHAPMAN LAYER MODEL

FIGURE 13

Table 4

Computed electron content for the region from 1000 Km to the F2 peak

	Total Electron Content (cm^{-2})					
	1	2	3	4	5	
Night-time profile	2.879	2.865	2.784	2.859	2.6798	$\times 10^{12}$
Day-time profile	12.112	11.969	11.887	12.037	12.065	$\times 10^{12}$

1 = Post Reduction

2 = Step-by-step

3 = Step-by-step with post reduction

4 = Iterative solution

5 = Linear method

4.2 A HIGH LATITUDE PROFILE

Reduction of Alouette high latitude ionograms requires more precise techniques than employed in other regions. The relatively low values of electron density at the satellite result in large ratios of f_h/f_x so that the group refractive indices will be quite sensitive to the variation of f_h with height.

The ionogram shown in Figure 14 was reduced by the iterative, post reduction, and linear laminations. Virtual heights were scaled at relatively wide intervals so that adequate frequency resolution could be obtained. The electron density profiles are shown together in Figure 15. The post reduction method gave true heights about 15 km lower than the iterative method except near the satellite where both were about the same. The linear method profile was much higher than the iterative one by about 50 km in the middle of the profile and about 35 km near the layer peak. Nighttime model studies have shown that when the ratio f_h/f_x is large at the satellite (it was 0.86 for this ionogram) that the linear method heights were well above those of the iterative method and that the situation is reversed for small ratios.

Electron density scale heights of these profiles are shown in Figure 16. Both the iterative and post reduction methods give similar results, and indicate a non-isothermal ionosphere with appreciable H_e^+ above 900 km. Linear method scale heights are generally lower except near the satellite and the layer peak.

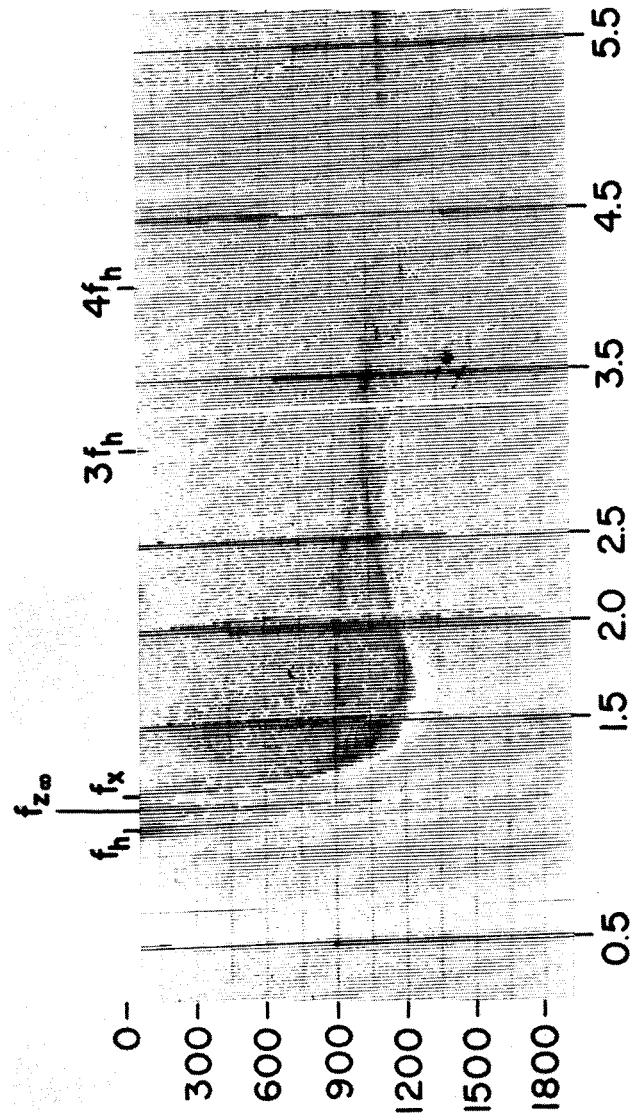

NOV. 29, 1962 , 12:03:30 GMT , 64.12°N, 61.86°W
HIGH LATITUDE ALOUETTE IONOGRAM

FIGURE 14

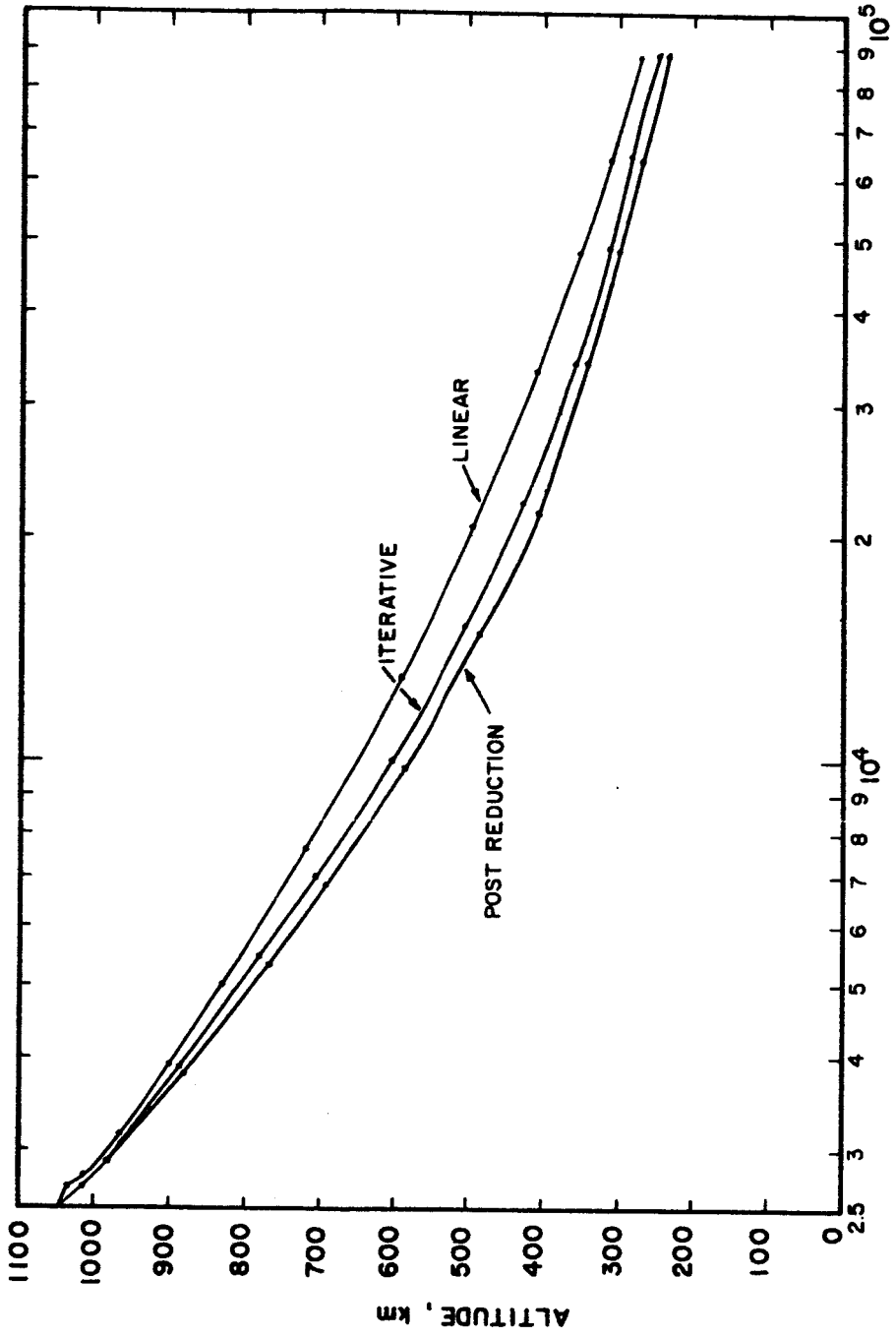

TRUE HEIGHTS CALCULATED FROM IONOGRAM IN FIGURE 14

FIGURE 15

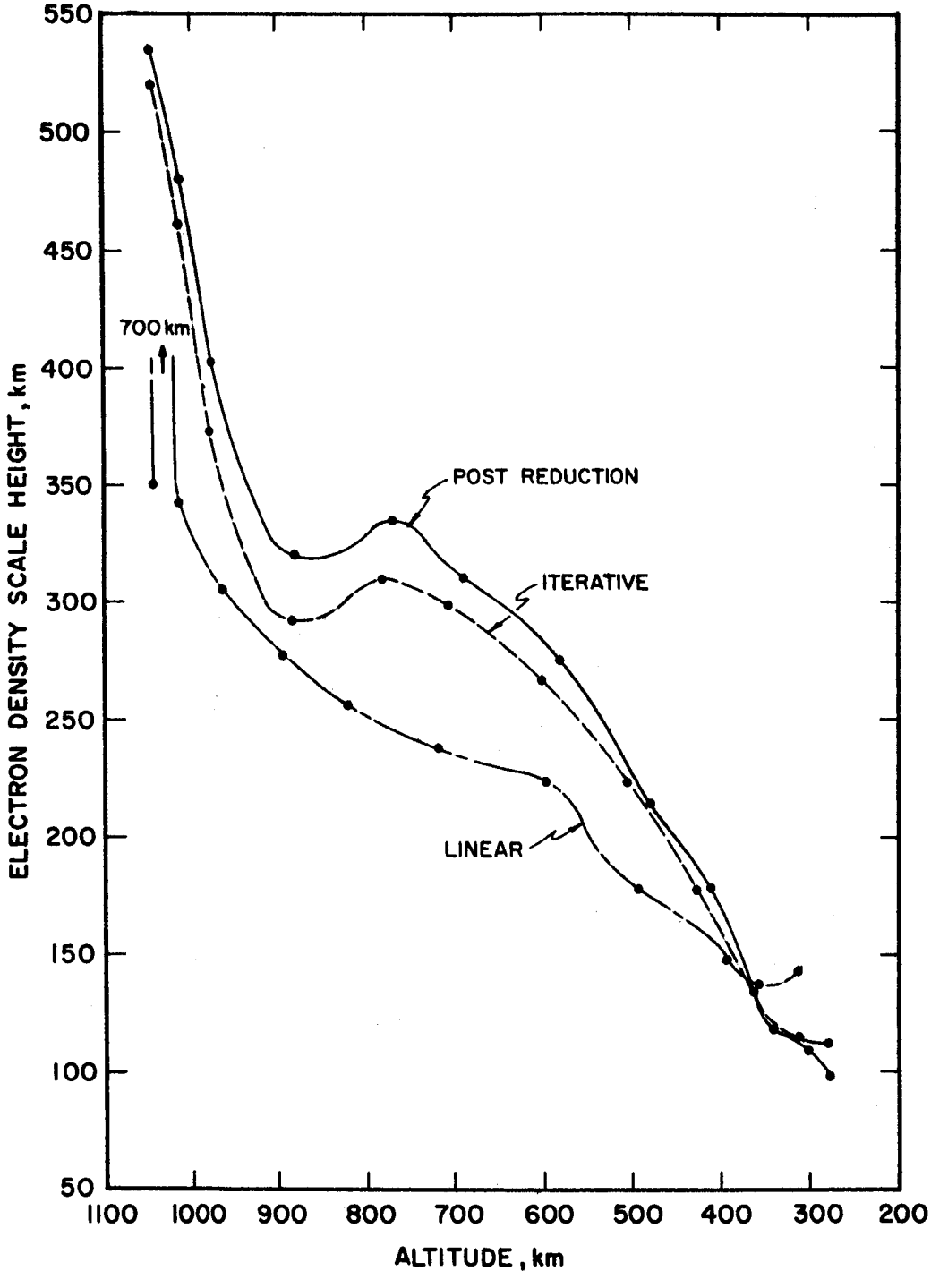

ELECTRON DENSITY SCALE HEIGHTS
COMPUTED FROM IONOGRAM IN FIGURE 14

FIGURE 16

Appendix 1 Evaluation of the Integrals in Equation (4).

Integrals of the form

$$I = \int_{f_{N_1}}^{f_{N_2}} \mu' \, df_N$$

must be calculated numerically because of the complicated integrand. Special precautions must be taken because μ' has a pole at the reflection level. The first of these is to obtain a numerically accurate formulation for μ' which is suitable for a digital computer. Following the notation of Ratcliffe (1959),

$$X = f_N^2/f^2$$

$$Y = f_h/f$$

and let $S = \sin \phi$

$$C = \cos \phi$$

where ϕ is the angle between the wave normal and the earth's magnetic field.

Starting from the collisionless Appleton-Hartree equation, the following expressions can be derived

$$\mu'_o = \frac{1}{\mu_o} \left\{ 1 - \frac{YC^2X}{S_o^2 [YS^2 + R]} \left[(1-X) - \frac{YS^2(1+X)}{R} \right] \right\}$$

$$\mu_o = \sqrt{1-X} \left\{ \frac{Y(1+C^2) + R}{Y(1+C^2) - YC^2X + R} \right\}^{\frac{1}{2}}$$

$$S_o = \frac{Y[\,1 + C^2(1 - 2X)\,] + R}{YS^2 + R}$$

$$R = \sqrt{Y^2S^4 + 4C^2\,(1-X)^2}$$

$$\mu'_x = \frac{1}{\mu_x}\left\{1 + \frac{X(1-S_x)}{2S_x^{\,2}}\left[1 + \frac{Y^2S^2}{R}\left(\frac{1+X}{1-X}\right)\right]\right\}$$

$$\mu_x = \sqrt{1-X-Y}\left\{\frac{(1+Y-X)(1-X)}{Y^2\left[\frac{(1-X)}{Y} - 1 + C^2X\right]}\left[\frac{2(1-X) - Y^2S^2 + YR}{2.(1-X)^2 - Y^2S^2 + YR}\right]\right\}^{\frac{1}{2}}$$

$$S_x = 2\left[\frac{(1-X) + Y^2\,(XC^2-1)}{2(1-X) - YS^2 + YR}\right]$$

It is easily seen that the poles occur because of the factors $1/\sqrt{1 - X}$ and $1/\sqrt{1-X-Y}$ in the ordinary and extraordinary modes; respectively. The remaining terms in both expressions for μ' are finite and well behaved. The major differences between these rather formidable expressions and those used by other workers are that the singular terms are shown explicitly and the remaining terms are numerically accurate.

For the ordinary mode, define an angle θ by

$$\sin^2\,\theta = X,\quad 0 \leq \theta \leq \pi/2.$$

Then changing the variables of integration to θ, we have

$$df_N = f \cos\,\theta\, d\,\theta\,,$$

and

$$\mu'_o \, df_N = f\mu'_o \, \sqrt{1 - X} \, d\theta ,$$

thus removing the pole from the integrand. Similarly, for the extraordinary mode,

$$\sin^2 \theta = \frac{X}{1-Y} , \quad 0 \leq \theta \leq \pi/2.$$

Then

$$df_N = f \sqrt{1-Y} \cos \theta \, d\theta .$$

But

$$\cos \theta = \sqrt{1-X-Y} \, / \, \sqrt{1 - Y}.$$

Therefore,

$$\mu'_x \, df_N = f\mu'_x \, \sqrt{1-X-Y} / \sqrt{1-Y} \, d\theta ,$$

and this pole is also removed. The reason for these particular forms for μ' is now evident. The singular terms can be removed before numerical calculations rather than relying on the digital computer to make accurate cancellations.

Let α' be the new integrand after removing the singular term,

$$\alpha'_o = f\left\{1 - \frac{YC^2X}{S_o^2[YS^2+R]}\left[(1-X) - \frac{YS^2(1+X)}{R}\right]\right\}\left\{\frac{Y(1+C^2)-YC^2X+R}{Y(1+C^2)+R}\right\}^{\frac{1}{2}}$$

$$\alpha'_x = f\left\{1+\frac{X(1-S_x)}{2S_x^2}\left[1+\frac{Y^2S^2}{R}\left(\frac{1+X}{1-X}\right)\right]\right\}\left\{\frac{(1+Y-X)(1-X)}{Y^2\left[\frac{(1-x)}{Y}-1+C^2X\right]}\left[\frac{2(1-X)-Y^2S^2+YR}{2(1-X)^2-Y^2S^2+YR}\right]\right\}^{\frac{1}{2}}$$

Many numerical integration formulas exist, but the one giving the highest accuracy with the fewest sample points is Gaussian quadrature (Kunz, 1957). In theory, other methods such as Simpson's rule would be suitable if more points were used. However, computational round-off errors become serious as the number of points is increased, and the computation time also increases. We have used a five or seven point Gauss-Legendre quadrature formula when integrating near the reflection level, and a three point formula elsewhere.

Appendix 2 Verification of Equation (7).

Consider M-1+N linearly independent equations in M+1 unknowns X, then

$$\underline{\underline{D}}\ \underline{X} = \underline{h'}$$

where D is an M-1+N by M+1 array of coefficients.

h' is an M-1+N column of data and

X is an M+1 column of unknowns.

The least squares solution requires that

$$\sum_{j=1}^{M-1+N} \sum_{k=1}^{M+1} (D_{jk}X_k - h'_j)^2$$

be a minimum with respect to each X.

Alternatively,

$$\frac{\partial \sum_{j=1}^{M-1+N} \sum_{k=1}^{M+1} (D_{jk}X_k - h'_j)^2}{\partial X_s} = 0 \quad \text{for } s = 1 \text{ to } M+1.$$

Therefore,

$$\sum_{j=1}^{M-1+N} 2 \sum_{k=1}^{M+1} (D_{jk}X_k - h'_j)\, D_{js} = 0 \quad \text{for } s = 1,\ M+1.$$

This gives M+1 independent equations in M+1 unknowns.

Now consider

$$\underline{\underline{D}}^t\ \underline{\underline{D}}\ \underline{X} - \underline{\underline{D}}^t\ \underline{h'} = 0.$$

Let

$$\underline{\underline{R}} = \underline{\underline{D}}^t \underline{\underline{h}} \quad \text{so that}$$

$$R_s = \sum_{j=1}^{M-1+N} D_{js}, h'_j, \qquad s = 1, M+1.$$

Define $\underline{\underline{E}} = \underline{\underline{D}}^t \underline{\underline{D}}$,

$$E_{sk} = \sum_{j=1}^{M-1+N} D_{js} D_{jk}, \quad s = 1, M+1; k=1, M+1.$$

Then

$$\underline{\underline{E}}\,\underline{\underline{X}} - \underline{\underline{R}} = 0$$

becomes

$$\sum_{j=1}^{M-1+N} \sum_{k=1}^{M+1} (D_{jk}X_k - h'_j)D_{js} = 0 \qquad \text{for } s = 1, M+1,$$

which is the desired least squares formulation.

References

Becker, W., Tables of Ordinary and Extraordinary Refractive Indices, Group Refractive Indices and h'o, x(f) Curves For Standard Ionospheric Layer Models, Max-Planck Institut fur Aeronomy, 4, 1960.

Brown, D. J., The Analysis of Ionospheric h'(f) Records Using the Method of Least Squares, Sci. Rpt. 202, Ionosphere Research Laboratory, Pennsylvania State University, 1963.

Budden, K. G., A Method For Determining the Variation of Electron Density With Height (N(Z) Curves) From Curves of Equivalent Heights Against Frequency ((h' ,f) Curves), Report Phys. Soc. Conf. on Physics of the Ionosphere, Cambridge, England, 332-339, 1954.

Chapman, J. H., Topside Soundings of the Ionosphere, Adv. in Astrn, Sci., 12, 1963.

Fitzenreiter, R. J. and L. J. Blumle, Analysis of Topside Sounder Records, J. Geophys. Res., 69, 407-416, 1964.

Hardy, J.D., An Investigation of the Influence of Collisions on Low Frequency Group Heights, Scientific Report 189, Ionosphere Research Laboratory, Pennsylvania State University, 1963.

King, J. W., P. A. Smith, D. Eccles, and H. Helm, The Structure of the Upper Ionosphere as Observed by the Topside Sounder Satellite Alouette, Radio Research Station document I.M. 94, 1963.

Kunz, K. S., Numerical Analysis, McGraw-Hill, New York, 1957.

Knecht, R. W., T. E. VanZandt, and J. M. Watts, The NASA Fixed Frequency Topside Sounder Program, in Electron Density Profiles, Vol. 2, 246, Pergamon Press, 1962.

Lanczos, C., Applied Analysis, Prentice Hall, 1956.

Paul, A. K., Bestimmung der Wahren aus der Schembaren Reflexionshohe, Arch. Elek. Ubertrag., 14, 468-476, 1960a.

Paul, A.K., Kritische Bemerkungen Zur Rerechnung der "Wahren Hohen", Geophys. Pura e Appl., 47, 69-78, 1960b.

Paul, A.K. and J. W. Wright, Some Results of a New Method for Obtaining Ionospheric N(h) Profiles With a Bearing on the Structure of the Lower F Region, J. Geophys. Res., 68, 5413-5420, 1963.

Ratcliffe, J. A., Magneto-ionic Theory, Cambridge Univ. Press, 1959.

Storey, L.R.O., The Joint Use of the Ordinary and Extraordinary Virtual Height Curves in Determining Ionospheric Layer Profiles, NBS J. of Res., 64D, 111-124, 1960.

Sulzer, P. G. and B. B. Underhill, Preliminary Vertical Incidence Equivalent Height Versus Time Recordings on 150 kc, Tech. Rpt. 8, Ionosphere Research Laboratory, Pennsylvania State University, 1949.

O'Brien, D. J. and W. J. Ross, Vertical Incidence Equivalent Height Recordings at 75 kc, Scientific Report 110, Ionosphere Research Laboratory, Pennsylvania State University, 1958.

Thomas, J. O. and A. R. Long, Titheridge Coefficients For the Polynomial Method of Deducing Electron Density Profiles From Ionograms, NBS J. of Res., 67D, 79-82, 1963.

Thomas, J. O. and D. Westover, The Calculation of Electron Density Profiles From Topside Sounder Ionograms Using a Digital Computer, Report SEL-63-130, Stanford Electronics Lab., Stanford University, 1963.

Titheridge, J.E., A New Method For the Analysis of Ionospheric h'(f) Records, J.A.T.P., 21, 1-12, 1961.

Van Meter, D., Vertical Incidence Equivalent Height Versus Time Recordings on 150kc., Technical Report 12, Ionosphere Research Laboratory, Pennsylvania State University, 1950.